JOURNAL OF CATALYSIS 62, 211–220 (1980)

Zinc-Deficient Zinc Aluminate-Supported Residual HDS Catalysts

JOHN. F. PATZER, II, WILLIAM L. KEHL, AND HAROLD E. SWIFT

Gulf Research & Development Company, P.O. Drawer 2038, Pittsburgh, Pennsylvania 15230

Received June 27, 1979; revised October 10, 1979

Eight zinc-deficient zinc aluminate supports are examined for initial activity in hydrodesulfurization of petroleum residues. Stoichiometric zinc aluminate, $ZnAl_2O_4$, has a spinel structure. The supports of this study, $Zn_xAl_2O_{3+x}$, $O < x < 1$, with insufficient zinc to form a true spinel structure, encompass a variety of defect spinel structures. The catalysts prepared from the supports are all active for sulfur removal from a Kuwait atmospheric tower bottom residue. Desulfurization activity, on a weight of catalyst basis, declines as zinc content of the support increases. Demetallization activity of the catalyst is adequately explained by the theory of restricted diffusion in catalyst utilization.

INTRODUCTION

Worldwide concern for the environment has prompted many nations to enact legislation directed toward control of sulfur oxide emissions. At the same time, a shifting crude oil availability pattern has trended toward more high sulfur crudes on the world market. In addition, the increasing price of crude oil makes it imperative to obtain as great a yield of low sulfur product as possible. The above considerations have led to the successful commercialization of residue hydrodesulfurization processes which catalytically remove sulfur from the high boiling point portion of crude oils as a preparative step for either direct combustion or further upgrading.

The direct desulfurization of petroleum residues constitutes the most difficult problem in petroleum desulfurization because contaminants which adversely affect catalyst performance are concentrated in the residue portion of the oil. Petroleum residue feedstocks are generally characterized by the substantial presence of asphaltenes, high carbon residues, and the presence of trace quantities of metal-containing compounds, mostly nickel and vanadium. Detailed discussions on the reactions of hydrodesulfurization and metals removal are available in the literature (*1–4*). Typically, the increased problems associated with processing of petroleum residues result from steric factors involved with large molecules depressing desulfurization reaction rates and deposition of metal contaminants on the catalyst surface reducing catalyst activity and effectiveness. The limiting factor in residual desulfurization catalyst life is the deactivation caused by accumulation of metals on the catalyst (*4*).

Typical hydrodesulfurization catalysts are composed of Group VIII metals in combination with a Group VIB metal, such as CoMo, NiMo, or NiCoMo, supported on alumina. A great deal of research has been expended in understanding how these metals complex with the alumina support to form active sites (*1, 12*). Surprisingly little knowledge, however, is available about the effects of utilizing supports other than alumina for residual hydrodesulfurization.

Zinc-Deficient Zinc Aluminate Supports

The structure of η-alumina resembles a defect spinel structure in which Al^{3+} ions are located in the interstices between O^{2-} ions in a close-packed oxygen lattice. This is a metastable structure because there are not enough cations available to form a proper spinel lattice, and, in particular, there are no divalent cations present to occupy the tetrahedral sites as in the nor-

0021-9517/80/040211-10$02.00/0

mal spinel structure. The Zn^{2+} ion has a very low octahedral site preference energy in comparison with Al^{3+}. Consequently, when Zn^{2+} ions are incorporated in the alumina structure, they will always occupy tetrahedral sites in the resulting spinel structure. The stoichiometric zinc aluminate spinel, $ZnAl_2O_4$, has a distinct lattice structure detectable by X-ray diffraction.

A zinc-deficient zinc aluminate spinel has a deficiency of zinc, $Zn_xAl_2O_{3+x}$, $O < x < 1$, relative to the stoichiometric spinel and is, thus, not a true spinel. While there is a net balance of positive and negative charges in the lattice, sites of locally unbalanced charge are expected to occur because of the zinc deficiency. This study examines the use of such zinc-deficient zinc aluminate spinels for use as a petroleum residue desulfurization catalyst support.

PROCEDURES

Preparation of Supports

The method of support preparation for this study consisted of precipitating the mixed hydroxides of zinc and aluminum from solutions of the nitrate salts with a mixture of NH_4OH and NH_4HCO_3. An approximately 1 *M* water solution of aluminum nitrate and zinc nitrate, in the desired proportions, was added slowly, with vigorous stirring, to a solution of NH_4OH and NH_4HCO_3. The pH of the mixing slurry was maintained constant in the range 9.0 to 9.5 throughout the precipitation by adding NH_4OH as needed. After all of the salt solution had been added, stirring was continued for 15 min to 2 hr, after which the precipitate was separated from the liquid by filtration. The filter cake was rinsed on the filter with distilled water to remove most of the residual ammonium nitrate. The filter cake was then broken up, dried in moving air at 120°C, and calcined at 500°C.

Eight zinc aluminate supports were prepared by the above method. Table 1 lists the supports and provides the relevant pore size properties of the supports as determined by the BET method. Figure 1 shows the X-ray diffraction patterns obtained for the calcined samples.

Support Impregnation

Active metals were deposited on each support by a double impregnation, incipient wetness technique. Molybdenum, from aqueous ammonium paramolybdate, was

TABLE 1

Pore Size Characteristics for Zinc-Deficient Zinc Aluminate Spinel Supports

	Support							
	S_1	S_2	S_3	S_4	S_5	S_6	S_7	S_8
Composition								
x in $Zn_xAl_2O_{3+x}$	0	0.1	0.1	0.3	0.5	0.8	0.8	0.8
BET properties								
Surface area (m^2/g)	286.1	236.7	245.5	203.2	208.1	198.6	209.6	205.9
Pore volume (cm^3/g)	0.81	0.39	0.43	0.30	0.37	0.23	0.23	0.19
Average pore radius (Å)	56.7	33.3	34.7	30.0	35.4	23.6	22.0	18.3
Median pore radius (Å)	83.1	36.2	41.2	34.0	44.5	24.8	22.5	19.6
Volume percentage of pore radii (Å)								
200–300	1.4	1.7	1.8	1.8	1.2	2.6	2.8	3.1
100–200	28.7	8.1	5.7	3.9	11.3	3.6	1.2	0.3
50–100	47.7	16.3	11.5	9.5	32.7	3.0	3.6	0.8
30–50	13.7	38.6	59.2	39.0	22.2	25.4	15.3	11.0
15–30	8.5	35.2	20.5	43.7	30.1	56.1	65.1	60.8
<15	0.0	0.2	1.2	2.1	1.7	9.4	11.9	23.9

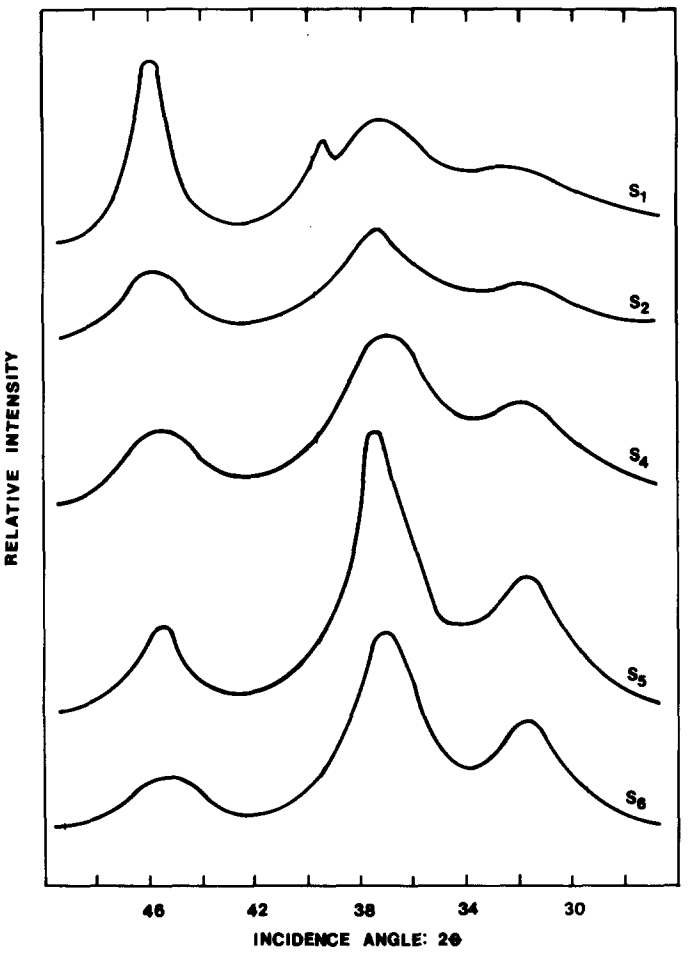

FIG. 1. X-Ray diffraction patterns for zinc-deficient zinc aluminate supports.

first impregnated onto the support material. The material was then oven dried at 120°C and subsequently calcined at 538°C. A second impregnation solution was prepared by dissolving appropriate amounts of $Co(NO_3)_2 \cdot 6H_2O$ and $Ni(NO_3)_2 \cdot 6H_2O$ in distilled water. The second impregnation solution was then used to impregnate the molybdenum-containing material. The catalyst was then oven dried at 121°C and subsequently calcined at 538°C. The nominal active metal concentrations were 1.3% CoO, 0.6% NiO, and 12.0% MoO_3, based upon total catalyst weight, for all eight catalysts. Table 2 gives the resultant pore size properties and packing density for each catalyst. Packing density is the mass of 595- to 841-μm-mean diameter particles which occupies 1 cm^3 when tapped to compaction.

Residue Desulfurization

Each catalyst was evaluated for initial activity in desulfurization of a Kuwait atmospheric tower bottom (ATB) residue in a continuous, single-pass trickle bed reactor. A catalyst bed consisting of 40 cm^3 of 595- to 841-μm-mean diameter particles was used for all experiments. The fresh catalyst was sulfided prior to an experiment by passing 3.8 mole/hr of an 8% H_2S–92% H_2 gas blend through the reactor, which was maintained at 204°C and atmospheric pressure, for a period of 2 hr. Evaluation conditions were 371°C, 6.89 mPag, 1.0 liquid

TABLE 2

Pore Size Characteristics for Zinc-Deficient Zinc Aluminate Spinel-Supported Catalysts

	Catalyst							
	A	B	C	D	E	F	G	H
Support	S_1	S_2	S_3	S_4	S_5	S_6	S_7	S_8
Packing density (g/cm³)	0.61	0.97	0.90	1.07	1.02	1.21	1.15	1.27
BET data								
Surface area (m²/g)	238.9	222.9	201.0	191.1	177.8	174.5	176.8	159.5
Pore volume (cm³/g)	0.50	0.31	0.37	0.24	0.26	0.17	0.21	0.16
Average pore radius (Å)	42.2	28.0	36.5	25.0	28.7	19.0	23.8	19.8
Median pore radius (Å)	59.1	30.6	44.0	27.7	32.9	20.5	25.2	21.5
Volume percentage of pore radii (Å)								
200–300	9.7	4.1	4.1	0.8	1.7	0.3	1.4	0.2
100–200	21.9	6.5	7.9	2.4	5.7	0.9	4.3	0.7
50–100	24.8	13.1	29.2	8.7	24.2	3.1	4.1	3.2
30–50	20.6	27.7	32.0	29.7	22.9	11.3	21.7	16.0
15–30	21.8	42.3	25.9	50.4	39.8	67.2	59.8	60.3
<15	1.2	6.4	0.7	8.0	5.8	20.3	8.6	18.4

hourly space velocity (volume of liquid/volume of catalyst bed/hr) and a hydrogen circulation rate of 37.6 kmole/m³ residue.

Catalysts A, B, D, E, and F were evaluated for 104 hr, with an initial offstream period of 8 hr, followed by 12 8-hr onstream periods. Catalysts C, G, and H were evaluated for 44 hr, with an initial offstream period of 8 hr, followed by four 8-hr and a final 4-hr onstream periods. The liquid product sulfur content was monitored for all onstream periods. In addition, the products from the 48 to 56-hr period for catalysts A, B, C, D, E, and F and the 40 to 44-hr period for catalysts C, G, and H were sampled for C, H, N, Ni, V, pentane insolubles, and Ramsbottom carbon residue. The results of the product analyses are shown in Table 3.

Reproducibility in product sulfur content for duplicate evaluations of a given catalyst, with the above reactor and experimental procedure, is ±0.05 wt% S for the product sulfur ranges encountered in this study. Although similar information is not available for the other product inspections obtained, it is assumed that the product inspection reproducibilities will be in the same relative range.

RESULTS

Catalyst Preparation

The presence of a spinel structure is readily detected through X-ray diffraction analysis. The X-ray diffraction patterns for supports S_1, S_2, S_4, S_5, and S_6, which have the nominal stoichiometry of $Zn_xAl_2O_{3+x}$, $x = 0$, 0.1, 0.3, 0.5, and 0.8, respectively, are shown in Fig. 1. The pattern for support S_1 is that of γ-alumina. This is not unexpected because alumina hydrates typically convert to γ-alumina upon calcination at the temperature used. X-ray diffraction of the oven-dried, but uncalcined, support S_1 showed the principal component to be bayerite.

The pattern for support S_2, $x = 0.1$, is quite similar to that of S_1 with little indication of zinc in the structure. The pattern for S_4, $x = 0.3$, however, shows the emergence of a peak at approximately $2\theta = 32$, which is indicative of the formation of detectable amounts of the spinel-type structure. This peak becomes more pronounced in the pat-

TABLE 3

Results o f Catalyst Evaluation at Specified Time On-Stream

		Catalyst							
	Kuwait ATB	A	B	C	D	E	F	G	H
Time on-tream (hr)		48–56	48–56	40–44	48–56	48–56	48–56	40–44	40–44
Product inspections									
C (wt%)	86.64	86.83	86.71	86.18	87.33	86.12	86.04	86.52	86.28
H (wt%)	11.47	11.90	11.83	12.29	12.04	11.85	11.85	12.06	12.05
S (wt%)	3.80	1.50	1.14	1.21	1.32	1.38	1.56	1.37	1.37
N (wt%)	0.20	0.20	0.18	0.20	0.18	0.19	0.19	0.20	0.17
Insolubles (wt%)	8.80	3.96	5.62	4.85	6.02	4.95	6.66	6.41	6.37
Carbon residue (wt%)	8.46	7.76	5.70	5.38	5.95	5.60	6.73	6.98	5.72
Ni (ppm)	15	9.1	11	7.1	9.6	8.2	11	9.0	11
V (ppm)	46	21	24	18	28	23	33	37	32
Desul furization rate constants									
k_{vs}[a]		40.4	61.4	56.3	49.4	46.1	37.8	46.7	46.7
k_{ws}[b]		63.3	60.5	59.8	44.1	43.2	29.8	38.8	35.1
k_{as}[c]		0.265	0.271	0.298	0.231	0.234	0.171	0.219	0.220

[a] $\left(\frac{\text{g oil}}{\text{gS-hr}}\right)\left(\frac{\text{cm}^3\text{ oil}}{\text{cm}^3\text{ catalyst}}\right)$.

[b] $\left(\frac{\text{g oil}}{\text{gS-hr}}\right)\left(\frac{\text{g oil}}{\text{g catalyst}}\right)$.

[c] $\left(\frac{\text{g oil}}{\text{gS-hr}}\right)\left(\frac{\text{g oil}}{\text{m}^2\text{ catalyst}}\right)$.

terns obtained for supports S_5 and S_6, $x = 0.5$ and $x = 0.8$, respectively.

The effects of incorporating zinc into the alumina lattice are also readily evident in the changing pore structure characteristics, as illustrated by Table 1. Replicate samples of $Zn_{0.1}Al_2O_{3.1}$, one replicate, and $Zn_{0.8}Al_2O_{3.8}$, two replicates, are provided to indicate the variance which can be expected in supports prepared by the methods of this study. Increasing zinc content in the support and, concomitantly, increasing formation of zinc aluminate spinel structure results generally in decreasing surface area, decreasing pore volume, and decreasing pore sizes. The shift in pore structure is most interesting. The alumina support, S_1, has a broad pore size distribution, as evidenced by the spread between the average pore radius and the median pore radius, 56.7 and 83.1 Å, respectively. However, as soon as zinc is incorporated into the structure, a nearly unimodal pore size distribution results, as shown by the generally small spread between the average pore radius and median pore radius. A considerable shift to smaller pore sizes occurs as the zinc content of the support increases, as seen by the decrease in average pore radius from the $Zn_{0.1}Al_2O_{3.1}$ support to the $Zn_{0.8}Al_2O_{3.8}$ support, about 33 and about 21 Å, respectively.

The general trends observed with the support pore structure characteristics carry over to the actual catalysts (Table 2). The effect of impregnation was to reduce the surface area and pore volume of the catalyst relative to the supports, most likely by occlusion of the finer pore structure by the deposited metals. It is interesting to note that the average pore radius and actual pore size distribution for the unimodal zinc-deficient zinc aluminate supports was largely unaffected by the impregnation. The

packing density, obtained for the catalysts, shows an increase in density with approach to stoichiometry in zinc content of the support.

Residue Desulfurization

The eight catalysts evaluated in this study were all active for desulfurization of the Kuwait ATB feedstock. The catalysts were also quite stable, with little evidence of aging over the length of an experiment, under the reaction conditions employed. The initial activity with time for catalysts A, B, D, E, and F is shown in Fig. 2 as a plot of product sulfur content versus time. The desulfurization level ranged from a high of approximately 68% for catalyst B to a low of approximately 57% for catalyst A by the end of an experiment. The product inspections, provided in Table 3, show that the zinc aluminate-supported catalysts perform similarly to conventional residue HDS catalysts (*4*).

DISCUSSION

The zinc-deficient zinc aluminate-supported catalyst system provides an opportunity to examine how changes in both the chemical and physical properties of a catalyst support can influence the major reactions of importance, namely, desulfurization and demetallization, in the conversion of petroleum residues. Considerable controversy exists in the patent literature as to the desirability of any given catalyst pore structure for residue desulfurization (*3*). Commercially important catalysts will be those which can maintain high sulfur removal activity over an acceptable life cycle despite the deactivation effects of contaminant metals desposition.

Desulfurization

The kinetics of hydrodesulfurization processes is complex. It is generally conceded that, while the intrinsic kinetics for individual sulfur-bearing compounds is first order, the overall, observed kinetics for hydrodesulfurization is second order (*5, 6*). The shift from first-order to observed second-order kinetics occurs because the wide spectrum of sulfur bearing species, with a corresponding wide distribution of activities, results in a lumped kinetic expression of overall order greater than unity (*7*).

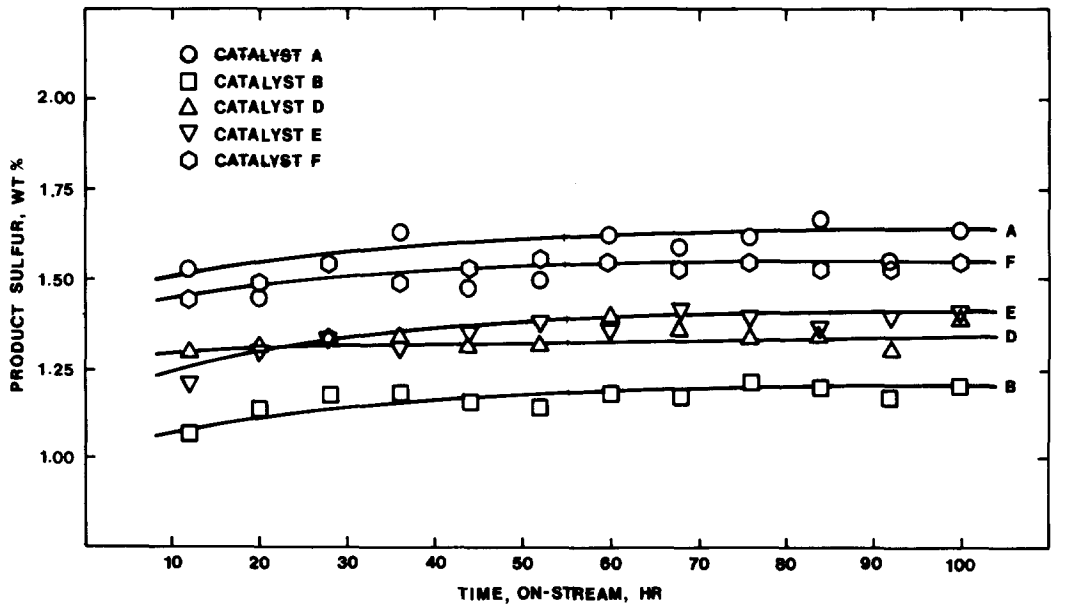

FIG. 2. Catalyst activity for desulfurization of Kuwait ATB.

An important consideration in residue hydrodesulfurization is whether restricted diffusion of large reactant molecules within the catalyst pore structure will affect catalyst utilization, as evidenced by a reduced effectiveness factor. The major portion of large molecules in a Kuwait residue which could primarily be affected by restricted diffusion are the asphaltenes. However, at desulfurization levels below about 70%, as employed in this study, asphaltenic sulfur remains largely unconverted (*3, 4*). Thus, reduced catalyst utilization would not be expected to be a problem for the desulfurization levels of this study. Shah and Paraskos (*2*) have shown catalyst effectiveness factors on the order of 0.9 for residue desulfurization can be expected for the reaction conditions employed in this study, thus confirming the expectation that restricted diffusion should not be important for sulfur removal.

Comparison of the zinc-deficient zinc aluminate-supported catalysts for desulfurization activity is straightforward. Three different second-order rate constants can be defined which highlight different aspects of catalyst performance: (i) a volume desulfurization rate constant, k_{vs}, (ii) a weight desulfurization rate constant, k_{ws}, and (iii) a surface area desulfurization rate constant, k_{as}. All three are tabulated in Table 3. The volume rate constant, k_{vs}, is commercially important because it compares catalyst performance under equal reactor volume conditions. This constant was rather erratic for the catalysts of this study due to different packing densities.

The weight rate constant and the surface area rate constants are more indicative of intrinsic catalyst activity. The weight rate constant compares catalysts on an equal amount of active metals basis while the surface area rate constant compares catalysts on a "turnover number" basis. The weight rate constants and surface area rate constants are plotted in Figs. 3a and b, respectively, as a function of zinc content in the support. The weight rate constant shows a definite decline in catalyst activity as the support zinc content increases. The surface rate constant, however, shows a peak in catalyst activity at a support zinc content of $Zn_{0.1}Al_2O_{3.1}$. These results imply that the most efficient use of active metals occurs with the alumina-supported catalyst while an intrinsically more active catalyst (molecules reacted/unit area) results when small amounts of zinc are incorporated into the alumina lattice.

Demetallization

The asphaltene model of residual oils pictures both nickel and vanadium atoms to be embedded in prophyrin structures. It is believed that vanadium atoms, as contrasted with nickel, are linked to an oxygen atom which is perpendicular to the plane of the porphyrin structure (*8*). The oxygen atom in the vanadium-bearing structure is believed to form a stronger link with the catalyst surface than can occur with the nickel-bearing compounds; consequently, leading to a higher vanadium removal rate than that of nickel. This qualitative view of the stereochemistry of the nickel- and vanadium-bearing species is borne out in the present study, with vanadium removal rates ranging from 0.74 to 3.25 times that of nickel, mostly greater than 1.4.

As previously discussed, restricted diffusion of asphaltene molecules should lead to a low catalyst utilization, or effectiveness factor, for metals removal. Shah and Paraskos (*2*) have estimated that the effectiveness factor for nickel and vanadium removal reactions is indeed low, not greater than about 0.4, for reaction conditions similar to this study. This being the case, the effect of varying pore structure should be apparent in the experimental results. Figure 4 presents a plot of percentage total demetallization versus catalyst average pore radius for the catalysts of this study where the actual demetallization data of Table 3 have been corrected to equivalent demetallization at 1 wt% S product utilizing sec-

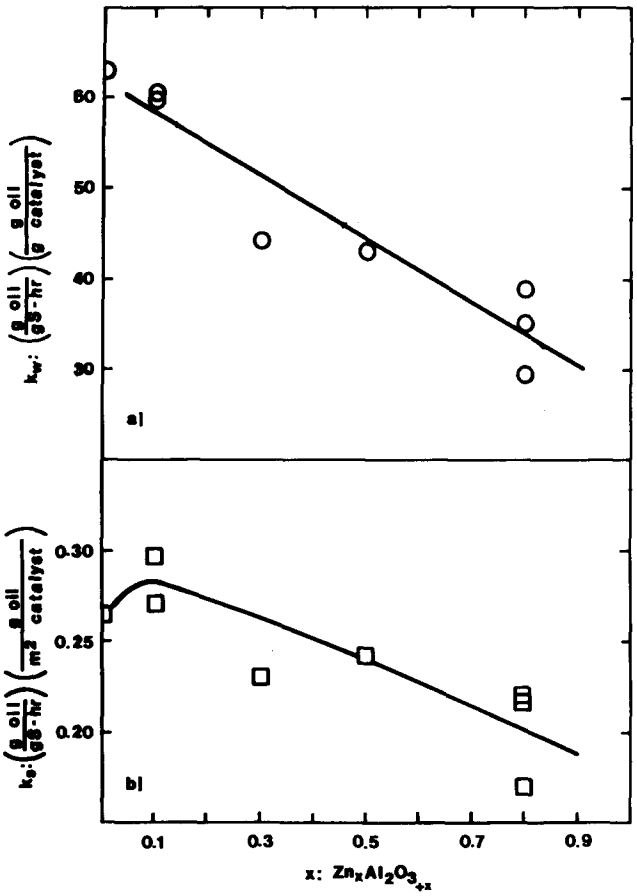

FIG. 3. Catalyst desulfurization rate constants as a function of support zinc content. (a) Weight rate constants; (b) Surface area rate constants.

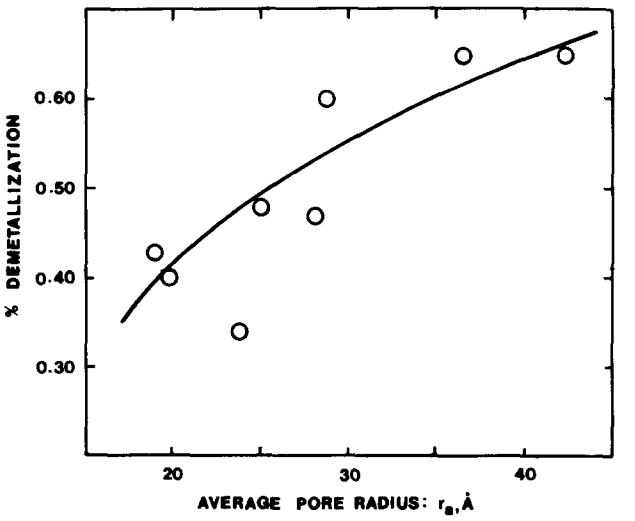

FIG. 4. Demetallization versus average pore radius at 1% S product.

ond-order kinetics. Linear regression of the data yields the relation

$$\%\text{deM} = -69.1 + 36.3 \ln r_a \quad (1)$$

with a correlation coefficient of 0.85.

Theoretical treatment of catalyst utilization shows the effectiveness factor, η, is asymptotically related to the Thiele modulus, ϕ, through the relation (*9*)

$$\eta = \frac{1}{\phi}, \qquad \phi > 3 \quad (2)$$

where

$$\phi = \frac{V_p}{S_x}\left(\frac{(n+1)kC_0^{n-1}}{2D_e}\right)^{1/2}$$

for particles of arbitrary shape. V_p is the particle volume, S_x is the particle external surface area, n is the order of the reaction, k is the intrinsic rate constant, and D_e is the species effective diffusion coefficient. For the purposes of this work, (2) can be rewritten as

$$\frac{\text{deM}}{(\text{deM})_0} = C_1\left(\frac{D_e}{k}\right)^{1/2} \quad (3)$$

where the effectiveness factor, η, has been rewritten as the ratio of the actual demetallization fraction, deM, to the maximum potential demetallization fraction in the absence of restricted diffusion, $(\text{deM})_0$, at 1 wt% sulfur product, and C_1 is a constant.

Two relevant correlations for restricted diffusion with respect to catalyst pore radius are available in the literature. Prasher and Ma (*10*) propose

$$D_e = A \exp\left(\frac{B}{r_a^3}\right); \qquad \lambda < 0.1 \quad (4)$$

and Satterfield *et al.* (*11*) propose

$$D_e = A \exp\left(\frac{B}{r_a}\right); \qquad 0.1 < \lambda < 0.5 \quad (5)$$

In (4) and (5), A and B are constants which depend on the solute unrestricted diffusivity and the catalyst pore structure, r_a is the catalyst average pore radius, and λ is the ratio of the solute geometric radius to the catalyst average pore radius. In the absence of other information, an assumption about the intrinsic rate constant for demetallization will be made that

$$k = \beta k_0 \quad (6)$$

where k_0 is some arbitrary rate constant and β is a number, dependent upon a particular catalyst, which when multiplied by k_0 gives the actual rate constant. The assumption will be that the relative β obtained for desulfurization weight rate constants are the same for demetallization.

Substitution of the expressions for D_e and use of (6) then yields, if (4) is used

$$ln[\beta(\text{deM})^2] \propto \left(\frac{1}{r_a}\right)^3 \quad (7a)$$

or, if (5) is used

$$Pn[\beta(\text{deM})^2] \propto \frac{1}{r_a}. \quad (7b)$$

Linear regression of the data with the suggested correlations, assuming $\beta = 1$ for catalyst A, found the best fit for (7b), shown in Fig. 5, with a correlation coefficient of -0.92. The best fit with (7b) should be expected because the large molecular size of asphaltenes, coupled with the relatively small pore structure of the zinc-deficient zinc aluminates, results in $\lambda > 0.1$.

The fit between the theory of restricted diffusion influence on catalyst utilization and the experimental results of this study is remarkable in view of the accuracy of the metals removal data, $\pm 10\%$, and the assumption about catalyst activity for metals removal paralleling catalyst activity for sulfur removal. The fact that restricted diffusion for demetallization is so apparent with these catalysts implies that they are probably susceptible to pore mouth plugging by metals deposits which would result in premature deactivation.

CONCLUSION

Zinc-deficient zinc aluminate supports are active for desulfurization of petroleum residues when impregnated with Group

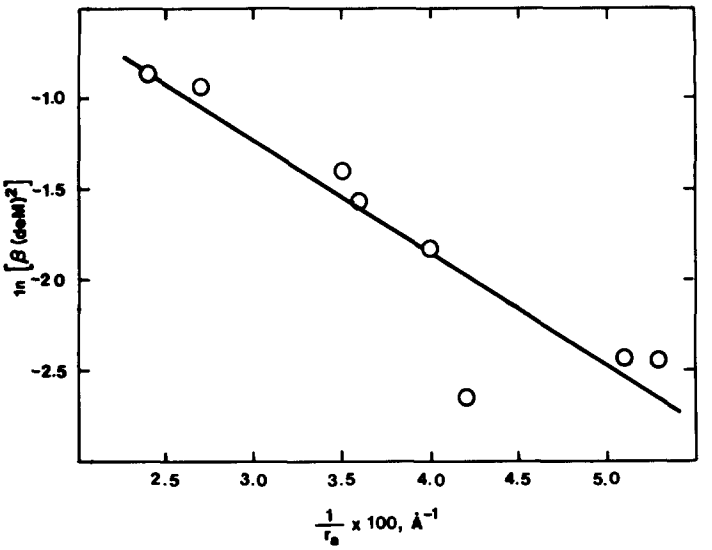

FIG. 5. Effectiveness factor correlation for demetallization versus average pore radius.

VIB and Group VII metals. The desulfurization activity, on a weight of catalyst basis, declines as the zinc content of the support approaches the stoichiometric spinel, $ZnAl_2O_4$. Metals removal activity is adequately explained by the restricted diffusion theory of catalyst utilization. As a result, it is believed that the supports will be subject to premature deactivation by pore mouth plugging due to metals deposition.

REFERENCES

1. Schuit, G. C. A., and Gates, B. C., *AICHE J.* **19**, 417 (1973).
2. Shah, Y. T., and Paraskos, J. A., *Ind. Eng. Chem., Process Des Dev.* **14**, 368 (1975).
3. Richardson, R. L., and Alley, S. K., *ACS Preprints, Div. Petrol. Chem.* **20**, 554 (1975).
4. Paraskos, J. A., Montagna, A. A., and Brunn, L. W., *AICHE Symp. Series* **72**, 127 (1972).
5. Beuther, H., and Schmid, B. K., Sixth World Petroleum Congress, Section III, Paper 20 (1963).
6. Yitzhaki, D., and Aharoni, C., *AICHE J.* **23**, 342 (1977).
7. Luss, D., and Hutchinson, P., *Chem. Eng. J.* **1**, 29 (1970); **2**, 172 (1971).
8. Dickie, J. P., and Yen, T. F., *Preprints, Div. Petrol. Chem. ACS* **12**, B-117 (1967).
9. Aris, R., *Chem. Eng. Sci.* **6**, 262 (1957).
10. Prasher, B., and Ma, Y. H., *AICHE J.* **23**, 312 (1977).
11. Satterfield, C. N., Colton, C. K., and Pitcher, W. H., Jr., *AICHE J.* **19**, 628 (1973).
12. Massoth, F. E., *in* "Advances in Catalysis" (P. D. Eley, H. Pines, and P. B. Weisz, Eds.), Vol. 27, p. 265. Academic Press, New York, 1978.